PKR deficiency alleviates pulmonary hypertension via inducing inflammasome adaptor ASC inactivation

Yapei Li[1], Ying Li[1], Lijun Li[2], Minghui Yin[2], Jiangang Wang[1] and Xiaohui Li[2,3] (iD)

[1]Department of Health Management Center, the Third Xiangya Hospital, Central South University, Changsha, China; [2]Department of Pharmacology, Xiangya School of Pharmaceutical Sciences, Central South University, Changsha, China; [3]Hunan Key Laboratory for Bioanalysis of Complex Matrix Samples, Changsha, China

Abstract

Pulmonary hypertension is a progressive fatal disease that currently has no specific therapeutic approaches. In this study, dsRNA-dependent protein kinase (PKR) was considered a candidate molecule in pulmonary hypertension. We demonstrated that PKR is activated in the endothelium of experimental pulmonary hypertension models. Deletion of PKR or treatment with the PKR activation inhibitor C16 inhibited the development of pulmonary hypertension. To explore the mechanism of PKR in pulmonary hypertension, we detected its downstream signaling and found that PKR knockout represses apoptosis-associated speck-like protein containing CARD (ASC) activation to inhibit high mobility group box 1 (HMGB1) and interleukin-1 beta release. To further explore whether ASC mediates the pro-pulmonary hypertension role of PKR, we used ASC deletion mice and found that ASC deletion inhibits the development of pulmonary hypertension and the release of HMGB1 and interleukin-1 beta. Furthermore, we co-cultured pulmonary arterial endothelial cells (PAECs) and pulmonary arterial smooth muscle cells (PASMCs) and found that endothelial PKR promotes PASMCs proliferation through the release of HMGB1 and interleukin-1 beta. In conclusion, these data indicate that endothelial PKR promotes the excessive proliferation of PASMCs by inducing ASC activation to release HMGB1 and interleukin-1 beta, which lead to the development of pulmonary hypertension. Our study will provide a novel insight that PKR is a potential target in the future treatment of pulmonary hypertension.

Keywords

Introduction

Pulmonary hypertension (PH) is a deadly disease characterized by occlusive pulmonary vascular remodeling, pulmonary artery pressure elevation and eventually death from right heart failure.[1,2] Abnormal pulmonary arterial endothelial cells (PAECs) function and pulmonary arterial smooth muscle cells (PASMCs) proliferation plays a leading role in occlusive vascular remodeling in PH.[3] The pathogenesis of PH is complex, multifactorial and highly interconnected. Immune inflammation is an essential contributor to the development of PH.[4,5] Classical inflammation had long been confirmed to participate in the occurrence of PH, but failed in clinical PH therapy. Non-classical inflammatory factor, including HMGB1 and IL-1β, has been considered as crucial therapeutic target of cardiovascular diseases in the recent years. Anti-inflammatory therapy targeting the interleukin-1β innate immunity pathway with canakinumab led to a significantly lower rate of recurrent cardiovascular

Corresponding authors:

Xiaohui Li, Department of Pharmacology, Xiangya School of Pharmaceutical Science, Central South University, 172 Tongzipo Road, Changsha 410013, China.
Email: xiaohuili@csu.edu.cn

Jiangang Wang, Department of Health Management Center, the Third Xiangya Hospital, Central South University, 138 Tongzipo Road, Changsha 410013, China.
Email: 600410@csu.edu.cn

diseases in clinical patient.[6] Our studies and others have revealed that several inflammatory factors, such as IL-1β and HMGB1, are significantly increased in clinical PH and play an important role to promote the PASMC proliferation in experimental PH.[7–11] However, it remains uncertain whether a crucial target links the intricate pathogenesis of PH, including inflammation and metabolic signaling.

Double-stranded RNA kinase (PKR) is a ubiquitously expressed type I interferon-induced serine/threonine protein kinase. It has traditionally been known to be activated during viral dsRNA infection and plays an important role in antiviral infection.[12] However, recent studies have shown that PKR can also be activated by endogenous substances and plays an important role in noninfectious diseases, including metabolic, immune and inflammatory diseases.[13–15] In our previous study, we found that PKR can be activated by palmitic acid in endothelial cells.[16] But the role of endothelial PKR in PH is still unknown.

It has been reported that PKR can recognize pathogenic-associated molecular patterns (PAMPs) or host-derived dangerous signal molecules (DAMPs) to take part in the course of innate immune defense through the inflammasome pathway.[17] PKR directly binds to NLRP1b, NLRP3 or NLRC4 inflammasome, which recruit inflammasome adaptor ASC to induce activation of inflammatory protease caspase-1 and release of IL-1β and HMGB1.[17,18] In addition, previous study highlighted that ASC knockout can inhibit hypoxia-induced PH and PASMC proliferation.[19] Therefore, we hypothesize that PKR can induce PH by initiating ASC-mediated inflammation.

Taken together, we hypothesize that endothelial PKR induces activation of ASC to release HMGB1 and IL-1β, which lead to the abnormal proliferation of PASMCs and then accelerate the development of PH.

Methods

Animals

Animal care and experiments were performed with approval from the animal ethics committees of our University, and all the experimental procedures were conducted in accordance with the guidelines for experimental animal use. PKR knockout and ASC knockout mice were kindly provided by Dr. Jianfeng Wu (Xiamen University, Xiamen, China). C57/B6L male mice (8–10 weeks old) were used as wild-type mice. Wild-type mice and gene knockout mice were used to construct the SU5416/hypoxia model. Sprague-Dawley rats (150–180 g) were used to establish the MCT model and the SU5416/hypoxia model.

MCT rat model

Sprague-Dawley rats were purchased from the Laboratory Animal Center of our University. Animals were randomly allocated into two groups. Control rats (n = 7) received intraperitoneal (i.p.) injections of saline as a vehicle control. The PH rats (n = 7) received a single i.p. injection of monocrotaline (MCT, 60 mg/kg, Sigma-Aldrich, USA). The animals were anesthetized by intraperitoneal application of sodium pentobarbital (50 mg/kg) and euthanized by CO_2 inhalation on the 21st day after the MCT injection for hemodynamic assessment. Lung tissues were obtained as described previously.[20] To obtain rat pulmonary artery, the pulmonary artery and pulmonary interstitial tissue were isolated from the proximal end to the distal end by blunt separation under stereomicroscope.

SU5416/hypoxia model

Sprague-Dawley rats (n = 6 in each group) were given a single i.p. injection of Sugen5416 (SU5416, 20 mg/kg, Selleck, USA) in vehicle (0.5% carboxyl methylcellulose sodium, 0.4% polysorbate 80, 0.9% benzyl alcohol), placed immediately into a 10% O_2 chamber and maintained in hypoxia for three weeks. C57 mice (8–10 weeks, n = 6 in each group) were given a single weekly i.p. injection of Sugen5416, placed immediately into a 10% O_2 chamber and maintained in hypoxia for three weeks. After three weeks in hypoxia, rats and mice were placed in a normoxic environment for five weeks to induce pulmonary hypertension. The animals were anesthetized by intraperitoneal application of sodium pentobarbital (50 mg/kg) and euthanized by CO_2 inhalation after the hemodynamic assessment.

The PKR inhibitor C16 in the PH rat model

The PKR inhibitor C16 (200 μg/kg, Selleck, USA) was administered to rats by i.p. injection one week before MCT (n = 6 in each group) or SuHx (n = 6 in each group) administration, and then by i.p. injection once a week until the end of the experimental time. The animals were anesthetized by intraperitoneal application of sodium pentobarbital (50 mg/kg) and euthanized by CO_2 inhalation after the hemodynamic assessment.

Assessment of hemodynamics and right ventricular hypertrophy

Measurements of hemodynamics and right ventricular hypertrophy were conducted as described previously.[20] Briefly, at the end of the treatment protocol, rats or mice were anesthetized with intraperitoneal pentobarbital, and then a right heart catheter (PE 50 tubing) was inserted through the right jugular vein for the measurement of right ventricular systolic pressure (RVSP) with fluid-filled force transducers (zero referenced at the hilum). Right ventricular hypertrophy was evaluated by determining the ratio of the right ventricle weight to the left ventricle and septum weight (RV/LV+S).

Immunohistochemistry

Lung tissues were fixed in formalin and then embedded in paraffin according to previously published methods. Lung hematoxylin-eosin staining was conducted as previously described.[21] Immunohistochemistry of tissue sections was performed with the following primary antibodies: anti-PKR (1:100, Abcam, USA), anti-p-PKR (1:100, Abcam, USA) and anti-alpha smooth muscle actin (α-SMA, 1:100, Sigma-Aldrich, USA).

ELISA

Serum or cellular supernatant levels of HMGB1 and IL-1β were measured with ELISA kits (HMGB1 ELISA kit, Shino-Test Corp., Kanagawa, Japan and IL-1β ELISA kit, R&D Systems, USA). The procedure was performed following the manufacturer's instructions described earlier.[22]

Cell culture

Human primary PAECs were purchased from ATCC and cultured in EBM (Lonza, USA) supplemented with 10% FBS. Human PASMCs were purchased from ATCC and cultured in primary smooth muscle cell medium (Lonza, USA) supplemented with 10% FBS. PAECs or PASMCs from passages 3 to 8 were used for all experiments. All cellular experiments were performed at least three times.

siRNA transfection

Human PAECs were maintained in serum-free medium and transfected with PKR siRNA or scramble siRNA using Lipofectamine 3000 transfection reagent (Invitrogen, USA) according to the manufacturer's instructions. The siRNA was synthesized by Ribio (China), and the PKR siRNA sequence used as follows: 5′CAAAUUAG CGUUGAGAUA dTdT 3′. Six hours after transfection, the cells were returned to normal culture medium for 48 h prior to the following treatment.

Co-culture experiments

Six-well plates with a 0.4-μm pore-sized filter were used according to the manufacturer's instructions. PAECs (5×10^5 cells/well) were seeded in the upper chamber and allowed to adhere overnight prior to the co-culture experiments. And 5×10^5 PASMCs/well were seeded in the bottom chamber. Before beginning the co-culture experiments, indicated PAECs were stimulated with or without TNF-α and were co-cultured with PASMCs to observe the change of PASMCs proliferation ability. Additionally, recombinant human HMGB1 and IL-1β proteins (R&D Systems, USA) were added into bottom chamber to observe the change of PASMCs proliferation ability. The proliferation capability of PASMCs was measured by cell counting plate assays after 48 h.

Cell immunofluorescence

Indicated PASMCs were seeded into 15-mm glass-bottomed cell culture dishes (NEST Biotechnology, China) and allowed to adhere overnight. After fixed with 4% paraformaldehyde (PFA), the cells were stained with Ki67 (ab16667, 1:100, Abcam, USA) and α-SMA (19245, 1:100, Cell Signaling Technology, USA) via overnight incubation. For nuclear staining, DAPI solution (1:100, Thermo Fisher Scientific, USA) was added and incubated for 5 min. The cells were visualized and photographed using a confocal microscope (Leica TCS SP8X & MP).

Western blotting

Western blotting was performed as described previously.[20] In brief, frozen tissues or cells were lysed with RIPA lysis buffer containing PMSF, protease and phosphatase inhibitors (Roche Diagnostics, Germany). Protein concentration was quantified using a BCA protein assay kit (Pierce, USA). Samples containing 30 μg of protein were separated by SDS-PAGE gels and transferred to PVDF membranes. The membranes were blocked with 5% fat-free milk before incubation with primary antibodies specifically recognizing PKR (ab32052, 1:1000, Abcam, USA), p-PKR (ab32036, 1:1000, Abcam, USA), HMGB1 (ab18256, 1:1000, Abcam, USA), ASC (AG-25B-0006, 1:1000, Adipogen, USA) and IL-1β (MAB201, 1:1000, R&D system, USA). Immunoreactivity was detected by an enhanced chemiluminescence system, and bands were scanned with a Bio-Rad Imager. Individual band intensity was determined with ImageJ software.

Statistical analysis

Data are presented in graphs as the mean ± SEM. One-way ANOVA was used for comparisons among groups. The significance of differences between two groups was assessed with unpaired two-tailed Student's t-test. $P < 0.05$ was considered to be significant.

Results

PKR activation is elevated in the pulmonary vessels of experimental PH models

We established experimental PH models by monocrotaline (MCT) or SU5416/hypoxia (SuHx) and observed increase of right ventricular systolic pressure (RVSP) and right ventricular hypertrophy (Fig. 1a–d). In addition, hematoxylin-eosin (H&E) staining showed obvious pulmonary vascular remodeling in the experimental PH group (Fig. 1g, h). The expression and activity levels of PKR in the pulmonary
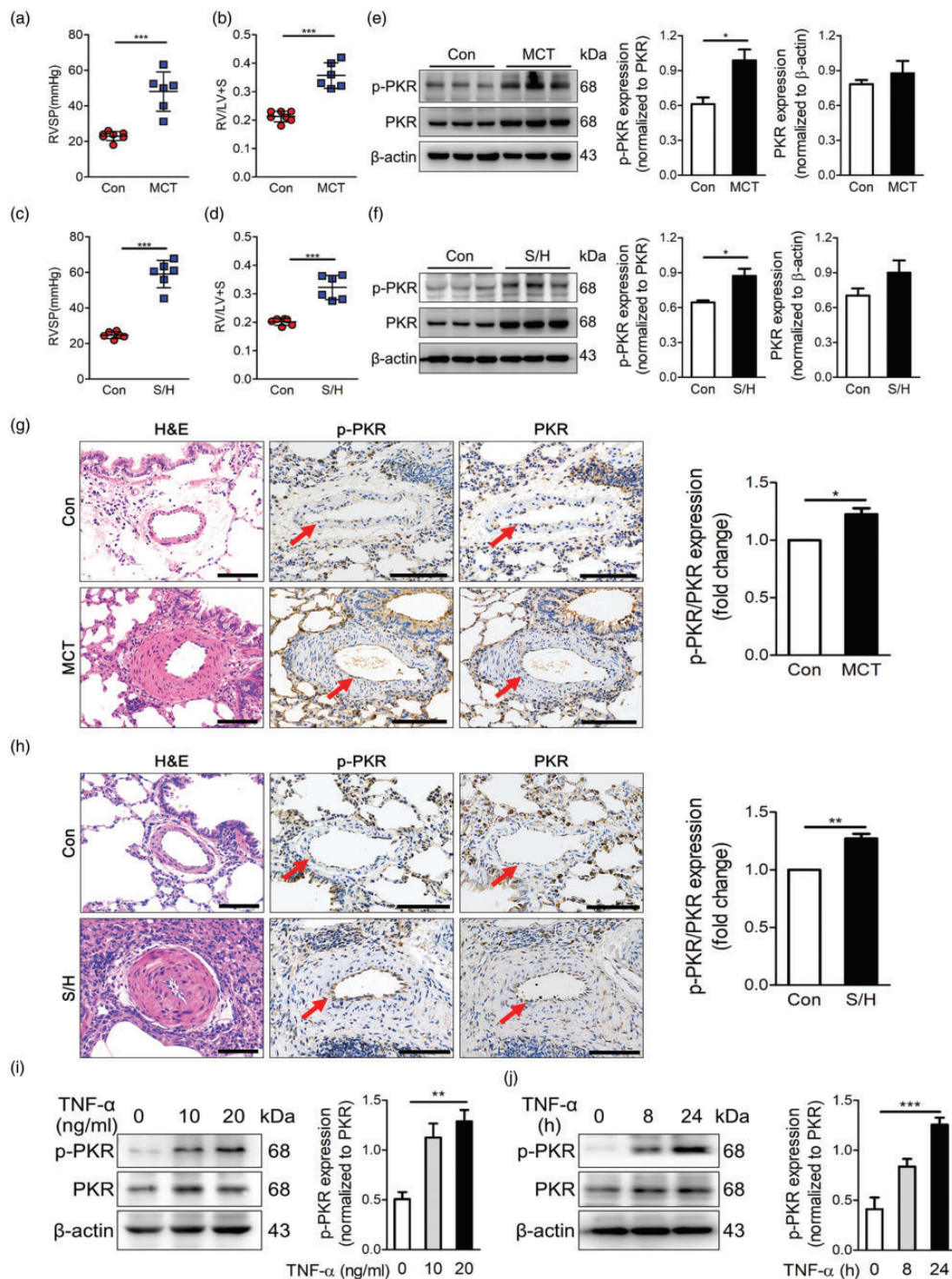
Fig. 1. PKR activation is elevated in the pulmonary vessels of experimental PH models. (a, b) Right ventricle systolic pressure (RVSP) (a) and indices of RV weight (RV/LV+S) (b) in rats given vehicle or MCT (60 mg/kg, i.p.) (n = 7). (c, d) Right ventricle systolic pressure (RVSP) measurements (c), indices of RV weight (RV/LV+S) (d) in vehicle and SU5416/hypoxia rats (n = 6). (e) Representative immunoblots and densitometric analysis of pulmonary artery PKR and p-PKR level in control and MCT rats (n = 3). (f) Representative immunoblots and densitometric analysis of pulmonary artery PKR and p-PKR level in control and SU5416/hypoxia rats (n = 3). (g) Photomicrographs of serial sections of peripheral rat lung containing small arteries from control animals and rats exposed to MCT rats. Sections were immunostained for the hematoxylin-eosin, PKR and p-PKR. Scale Bar = 25 μm. (h) Photomicrographs of serial sections of peripheral rat lung containing small arteries from control animals and SU5416/hypoxia rats. Sections were immunostained for the hematoxylin-eosin, PKR and p-PKR. Scale bar = 25 μm. (i) Representative immunoblots and densitometric analysis of PKR activation level was assessed in PAECs with TNF-α at 0, 10 and 20 ng/ml (n = 4). (j) Representative immunoblots and densitometric analysis of PKR activation level in PAECs under the treatment of TNF-α (20 ng/ml) for 0, 8 and 24 h (n = 4). $*P < 0.05$, $**P < 0.01$, $***P < 0.001$, by one-way ANOVA relative to control groups.

arteries of experimental PH rats and control rats were determined by immunoblotting. Activated PKR levels were low in normal pulmonary arteries significantly increased in those from PH rats (Fig. 1e, f). Moreover, immunohistochemical staining of lung tissue demonstrated that activated PKR expression was specifically increased in the endothelial cell of small-middle pulmonary arteries from PH rats (Fig. 1g, h). To further determine whether PKR activation is increased in PAECs) during challenge with a pro-PH stimulus, we stimulated human PAECs with the pro-PH inflammatory factor tumor necrosis factor-α (TNF-α) and found that TNF-α increased the activity of PKR both in a time- and dose-dependent manner (Fig. 1i, j).

PKR inhibitor is sufficient to abolish the development of experimental PH

To explore whether pharmacological PKR inhibitor prevents the development of pulmonary hypertension, rats were randomly assigned to receive the PKR inhibitor C16 or vehicle before an intraperitoneal injection of MCT to induce PH (Fig. 2a). The vehicle-treated rats developed PH, as shown by elevated right ventricular systolic pressure (RVSP) (Fig. 2b) and increased right ventricular hypertrophy (Fig. 2c). However, the PKR inhibitor C16-treated rats exhibited decreased levels of RVSP and right ventricular hypertrophy (Fig. 2b, c). For the reason that the excessive proliferation of PASMC-induced pulmonary vascular
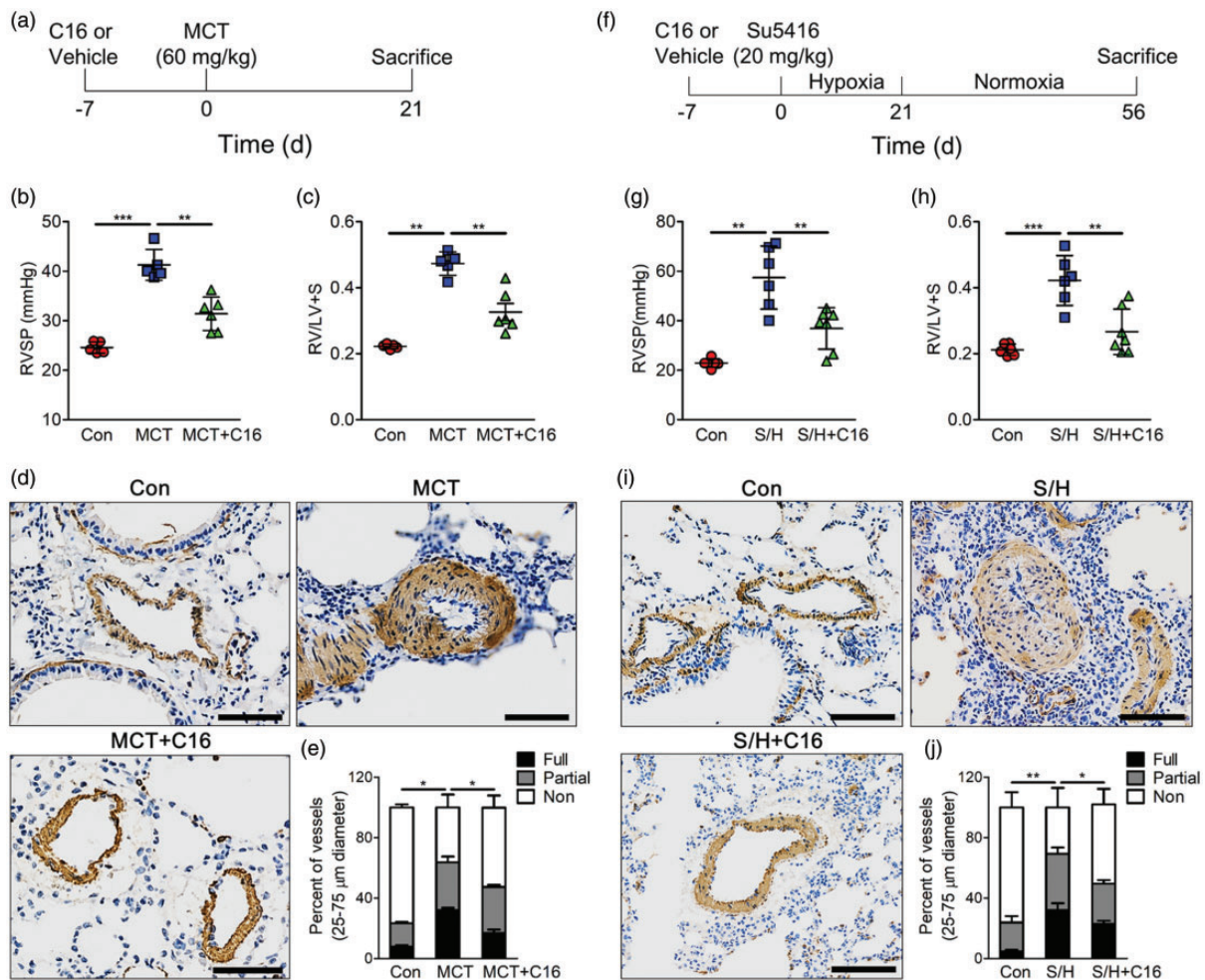

Fig. 2. PKR inhibitor is sufficient to repress the development of experimental PH. (a) Experimental timeline, (b–c) bar charts showing right ventricle systolic pressure (RVSP) (b) and indices of RV weight (RV/LV+S) (c) in control, MCT and C16 prevention groups (n = 6). (d) Photomicrographs of serial sections of peripheral rat lung containing small arteries from control, MCT and C16 prevention groups. Sections were immunostained for the α-SMA. Top scale bar = 50 μm. (e) Quantitative assessment of pulmonary arterial muscularization in control, MCT and C16 prevention groups. (f) Experimental timeline. (g–h) Bar charts showing right ventricle systolic pressure (RVSP) (g) and indices of RV weight (RV/LV+S) (h) in control, SU5416/hypoxia and C16 prevention groups (n = 6). (i) Photomicrographs of serial sections of peripheral rat lung containing small arteries from control, SU5416/hypoxia and C16 prevention groups. Sections were immunostained for the α-SMA. Top Scale Bar = 50 μm. (j) Quantitative assessment of pulmonary arterial muscularization in control, Su5416/hypoxia and C16 prevention groups. *$P < 0.05$, **$P < 0.01$, ***$P < 0.001$ by one-way ANOVA relative to Con or the indicated group.
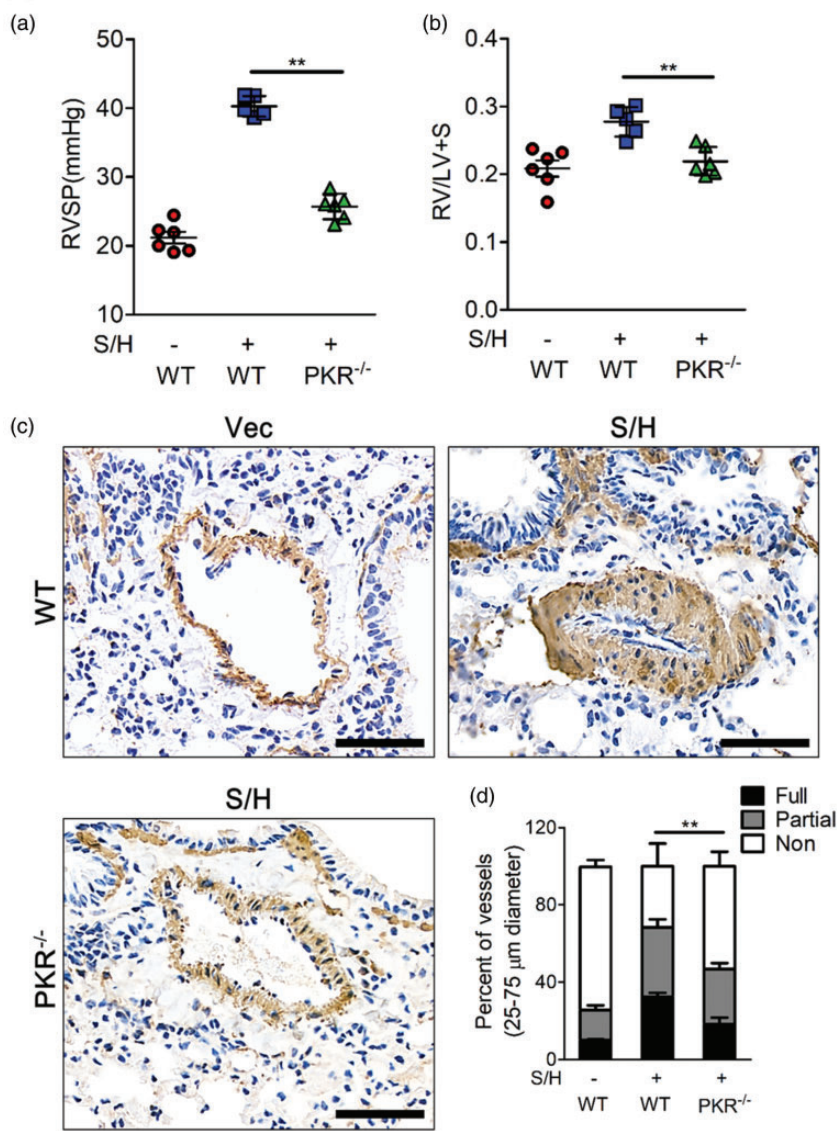
Fig. 3. Knockout of PKR inhibits SU5416/hypoxia-induced PH. (a–b) Right ventricle systolic pressure (RVSP) (b) and indices of RV weight (RV/LV+S) (c) in wild-type (WT) mice and PKR knockout mice after stimulation with SU5416/hypoxia (n = 6). (c) Photomicrographs of serial sections of peripheral mouse lung containing small arteries from wild-type mice and PKR knockout mice after stimulation with SU5416/hypoxia. Sections were immunostained for the α-SMA. Top scale bar = 200 μm. Bottom Scale Bar = 50 μm. (d) Quantitative assessment of pulmonary arterial muscularization in wild-type mice and PKR knockout mice after treatment with SU5416/hypoxia. **$P < 0.01$ by one-way ANOVA relative to wild-type mice treated with Su5416/hypoxia.

remodeling is a classic characteristic of PH, we detected the smooth muscle marker α-SMA in lung tissues to assess the remodeling of the small pulmonary artery. MCT induced massive pulmonary arterial muscularization, and the PKR inhibitor C16 prevented this effect (Fig. 2d, e). Since a monocrotaline rat model cannot fully replicate the pathology of PH patients, animals were treated with SU5416 via i.p. injection and subjected to three weeks of hypoxia followed by an additional five weeks in normoxia to establish a model of more severe PH (Fig. 2f). The hemodynamic and pathological parameters measured in the vehicle group indicated the development of PH (Fig. 2g–j). However, rats

treated with the PKR inhibitor C16 also exhibited decreased RVSP, right ventricular hypertrophy and pulmonary arterial muscularization (Fig. 2g–j). Taken together, these results suggested that inhibiting PKR activation can prevent the development of PH.

Knockout of PKR inhibits SU5416/hypoxia-induced PH

To further detect whether PKR specifically participates in the development of PH, we also established a SuHx model in PKR knockout mice. While the wild-type mice showed an
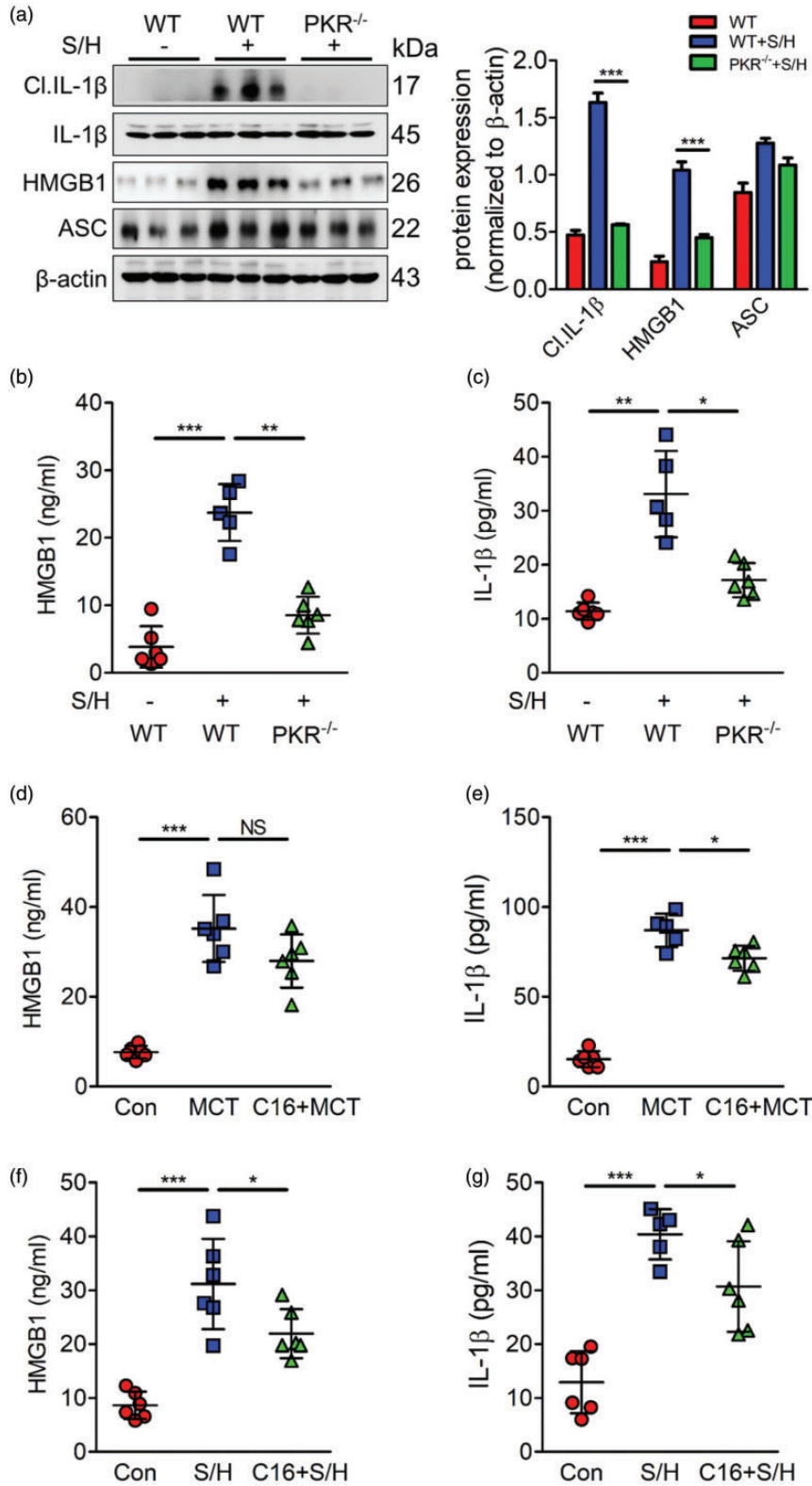
Fig. 4. PKR deletion represses ASC activation expression to inhibit HMGB1 and IL-1β release. (a) Representative immunoblots and densitometric analysis of pulmonary PKR and its downstream molecules, including ASC and mature IL-1β expression in wild type, SU5416/hypoxia, and PKR knockout mice after treatment with SU5416/hypoxia (n = 3). (b, c) Bar charts showing HMGB1 (b) and IL-1β (c) release into the plasma of wild type, SU5416/hypoxia, and PKR knockout mice treated with Su416/hypoxia (n = 6). (d, e) Bar charts showing HMGB1 (d) and IL-1β (e) release into the plasma of Con, MCT, and PKR pharmacological inhibitor C16 prevention group (n = 6). (f, g) Bar charts showing HMGB1 (f) and IL-1β (g) release into the plasma of Con, SuHx, and PKR pharmacological inhibitor C16 prevention group (n = 6). **$P < 0.01$, ***$P < 0.001$ by one-way ANOVA relative to control groups or the indicated group.
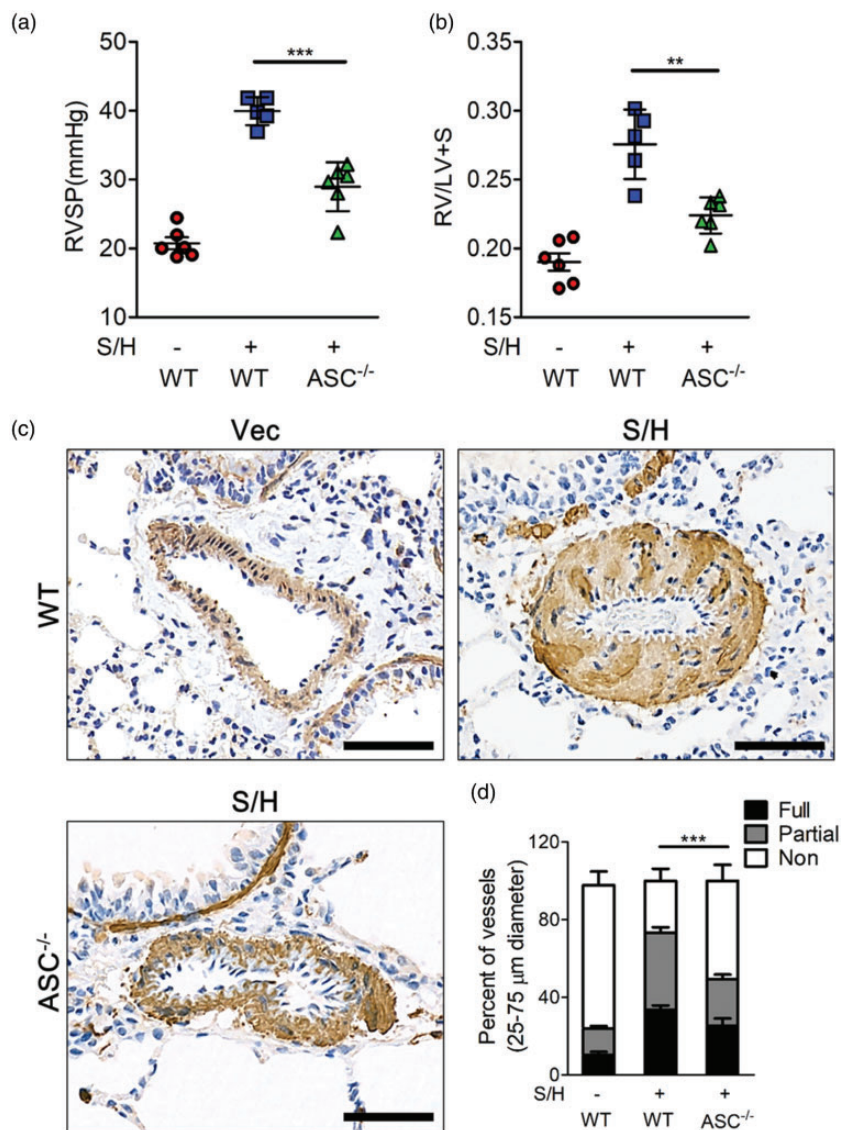
Fig. 5. Knockout of ASC can effectively inhibit the development of SuHx-induced PH. (a, b) Bar charts showing right ventricle systolic pressure (RVSP) (a) and indices of RV weight (RV/LV+S) (b) in wild-type mice and ASC knockout mice, and all of the above groups stimulated with SU5416/hypoxia (n = 6). (c) Photomicrographs of serial sections of peripheral mice lung containing small arteries from the above groups of mice. Sections were immunostained for the α-SMA. Scale Bar = 50 μm. (d) Quantitative assessment of pulmonary arterial muscularization in the above groups. *P < 0.05, **P < 0.01, ***P < 0.001 by one-way ANOVA relative to SU5416/hypoxia.

enhanced PH phenotype, PKR knockout mice exhibited healthier state, as shown by decreases in right ventricular systolic pressure, pulmonary vascular remodeling and right ventricular hypertrophy (Fig. 3a, b). In addition, immunohistochemical staining showed that PKR knockout inhibited the abnormal remodeling and muscularization of pulmonary arteries (Fig. 3c, d).

PKR deletion represses ASC activation to inhibit HMGB1 and IL-1β release

Previous studies have reported that PKR can bind to several inflammasomes, including NLRP3, NLRC4 and NLRP1b, to further induce inflammasome activation. ASC, the common adaptor of the inflammasome, is necessary for the assembly of the inflammasome and the cleavage of caspase-1 to induce the release of mature IL-1β and HMGB1, which have been confirmed to be important pathological factors in PH. Herein, we postulated that ASC is important downstream target of PKR in PH. Although the expression of ASC did not markedly change in PH mice, HMGB1 and IL-1β, as the downstream targets of ASC, were activated in the PH group (Fig. 4a). PKR deficiency inhibited the activation of ASC, detected by the decrease of HMGB1 and IL-1β (Fig. 4a). Moreover, we performed ELISA assay to assess the levels of HMGB1 and IL-1β in mice blood serum. Similar to the Western blotting results, in the PH models, HMGB1 and IL-1β release levels were much
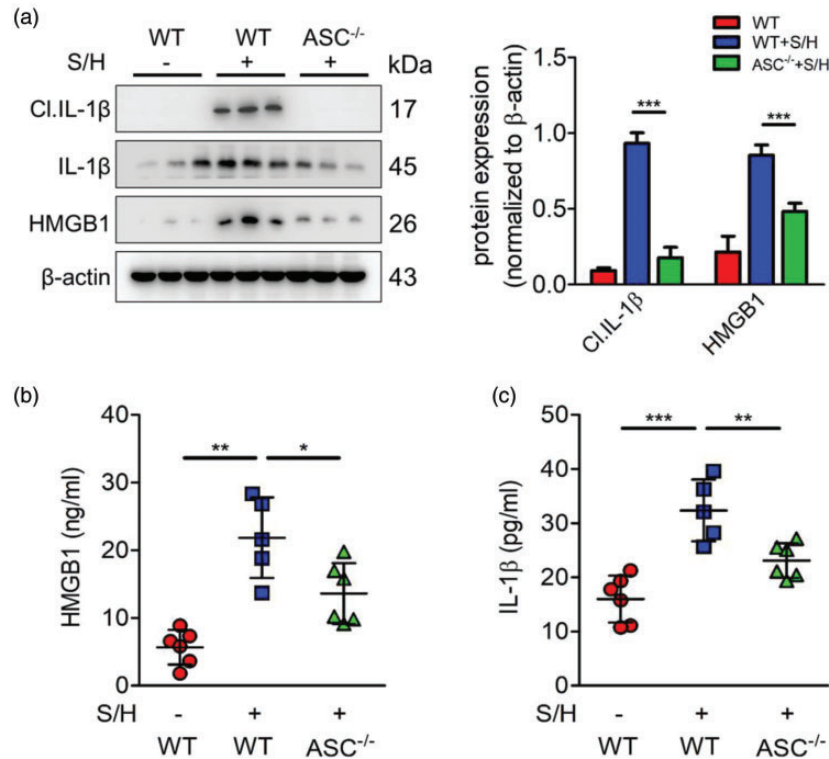
Fig. 6. ASC deletion represses HMGB1 and IL-1β release in PH model. (a) Representative immunoblots and densitometric analysis of pulmonary PKR and its downstream molecules, including ASC and mature IL-1β expression in wild type, SU5416/hypoxia, and ASC knockout mice after treatment with SU5416/hypoxia (n = 3). (b, c) Bar charts showing HMGB1 (b) and IL-1β (c) release into the plasma of wild type, SU5416/ hypoxia, and ASC knockout mice treated with Su416/hypoxia (n = 6). *P < 0.05, **P < 0.01, ***P < 0.001 by one-way ANOVA relative to control groups or Su5416/hypoxia group.

higher than those in the control group; however, this phenotype was prevented by PKR knockout (Fig. 4b, c). Furthermore, we also explore whether pharmacological PKR inhibitor C16 can prevent the release of HMGB1 and IL-1β. Our results showed that the levels of HMGB1 and IL-1β were also elevated in MCT or SuHx-PH rats. Performing PKR inhibitor C16 partially repressed this phenomenon (Fig.4d–g). These results suggest that PKR may promote the development of PH by regulating ASC -mediated inflammation.

Knockout of ASC effectively inhibits the development of severe PH

Although previous studies reported that knockout of ASC represses hypoxia-induced PH,[19,23] whether ASC deletion is sufficient to inhibit severe PH development is still unknown. Hence, we established SuHx PH models in ASC knockout mice or in the wild-type mice. Compared to the PH wild type mice, knockout of ASC showed decreased right ventricular systolic pressure (Fig. 5a), right ventricular hypertrophy (Fig. 5b) and pulmonary small vessel muscularization (Fig. 5c, d), which is similar with PKR knockout mice.

Knockout of ASC effectively inhibits HMGB1 and IL-1β release

Moreover, we detect whether ASC knockout also inhibits the activation and release of HMGB1 and IL-1β in PH models. Consistent with previous result, Western blotting showed that ASC deficiency inhibited the expression and activation of HMGB1 and IL-1β (Fig. 6a). We also performed ELISA assay to assess the levels of HMGB1 and IL-1β in mice blood serum. Similar to the Western blotting results, HMGB1 and IL-1β release levels were much higher in the PH models than those in the control group; however, this phenotype was prevented by ASC knockout (Fig. 6b, c). These results suggest that ASC promotes the development of PH by regulating HMGB1 and IL-1β release.

Endothelial PKR promotes HMGB1 and IL-1β release to induce the abnormal proliferation of PASMCs

Having demonstrated that PKR is specifically activated in the endothelial cell of pulmonary vessels in different PH rodent models and that knockout of PKR is sufficient to inhibit the development of PH, we next explored whether
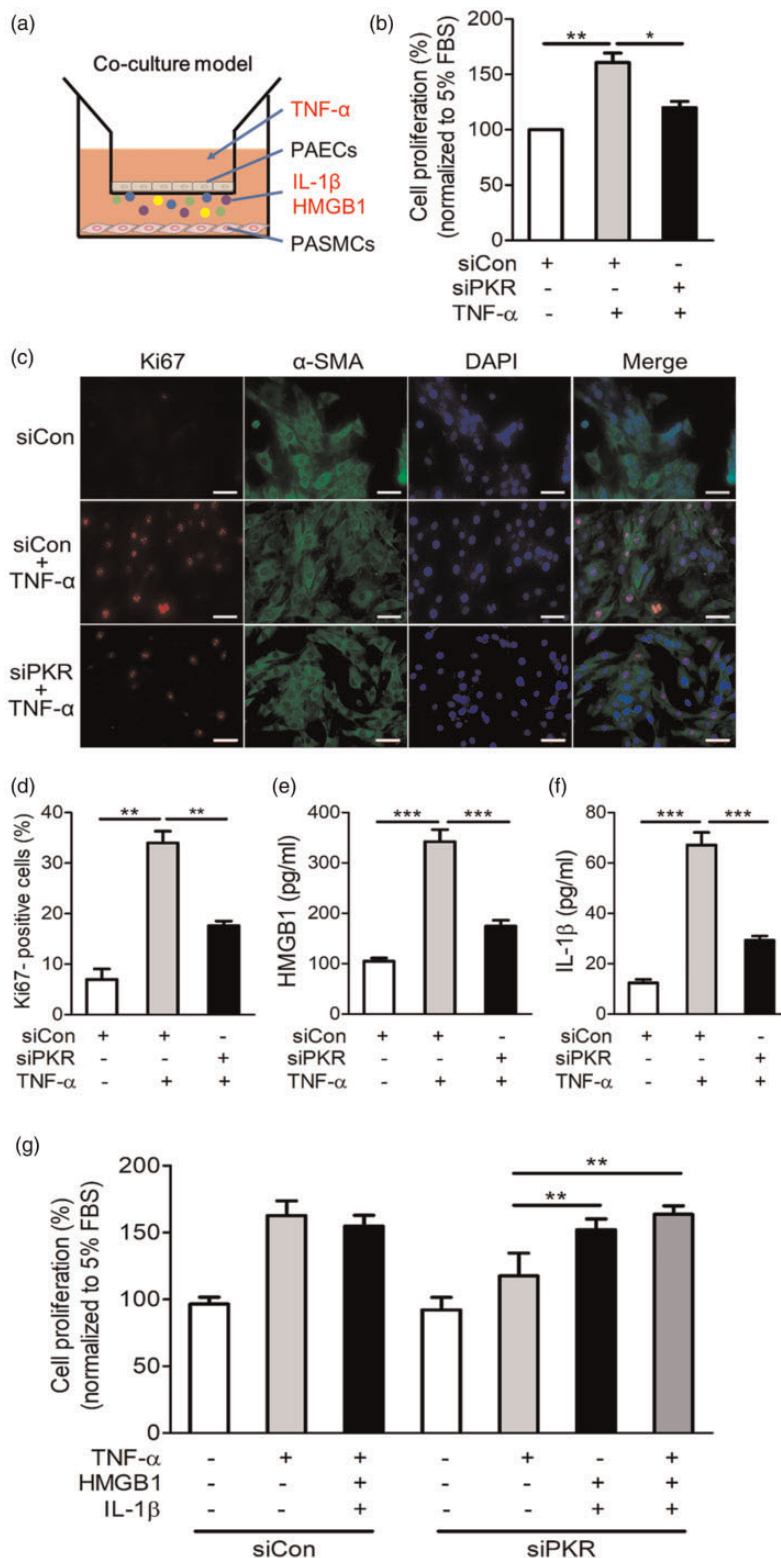
Fig. 7. Knockdown of PKR in PAECs prevents the abnormal proliferation of PASMCs. (a) The diagram of co-culture system. (b) In the co-culture system, PAECs were transfected with negative control siRNA (siCon) or PKR siRNA (siPKR) and then stimulated with TNF-α, CCK8 measures the proliferation ability of PASMCs (n = 3). (c) PASMCs were analyzed by immunofluorescence for the expression of Ki67 (red), α-SMA (green) and nuclei (DAPI, blue) in the indicated groups. (d) Bar charts showing the percentage of Ki67-positive PASMC (n = 3). (e, f) The release of HMGB1 (e) and IL-1β (f) by indicated PAECs (n = 6). (g) In the co-cultured system, PAECs were transfected with siCon or siPKR, and then stimulated with TNF-α. Simultaneously, PASMCs were treated with vehicle or recombinant HMGB1 and IL-1β, and the proliferation of PASMCs were analyzed by CCK8 and the percentage of cell proliferation was shown in the bar charts (n = 3).
*$P < 0.05$, **$P < 0.01$, ***$P < 0.001$ by one-way ANOVA relative to the control group.
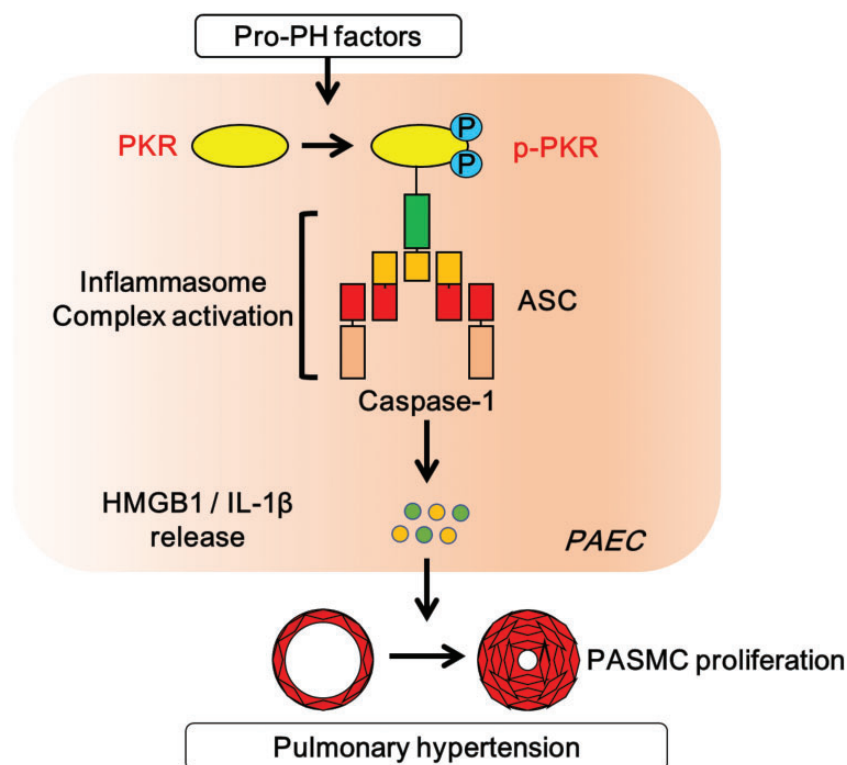
Fig. 8. A schematic representation of proposed mechanism for the role of PKR in PH development. Exposure to pro-PH factor TNF-α induces the activation of PKR in PAECs. Subsequently, phosphorylated PKR induces inflammasome adaptor ASC activation. This process promotes the release of inflammatory factors HMGB1 and IL-1β, which leads to the pulmonary artery smooth muscle cell excessive proliferation, and finally triggers the development of PH.
PAEC: pulmonary artery endothelial cell; PASMC: pulmonary artery smooth muscle cell.

activated PKR in PAECs is associated with abnormal PASMC proliferation. We co-cultured primary PAECs with PASMCs to evaluate the pro-proliferation role of endothelial PKR on PASMCs (Fig. 7a). We silenced PKR expression by siRNA in PAECs, then stimulated PAECs with TNF-α and co-cultured with PASMCs. Our results showed that PASMC proliferation ability was significantly increased while co-cultured with TNF-α-stimulated control PAECs (Fig. 7b). In addition, PASMC that co-cultured with TNF-α-stimulated control PAECs showed strong positive staining of Ki67, a marker of excessive cell proliferation (Fig. 7c, d). However, silencing PKR in TNF-α-stimulated PAECs blocked the abnormal proliferation and Ki67-positive staining of PASMCs (Fig. 7b–d). To further determine whether PKR in PAECs promotes PASMC proliferation via the release of HMGB1 and IL-1β, we detected the levels of HMGB1 and IL-1β in the cell supernatant. The results showed that the release of HMGB1 and IL-1β by PAECs increased after TNF-α stimulation; however, this phenomenon was abolished by PKR knockdown (Fig. 7e, f). Moreover, we found that the proliferation ability of PASMCs was significantly increased after stimulation with recombinant HMGB1 and IL-1β proteins, and this effect was similar to the effect of incubation with TNF-α (Fig. 7g). Knockdown of PKR in PAECs did

not abolish the pro-proliferative role of HMGB1 and IL-1β recombination proteins on PASMCs (Fig. 7g). Taken together, these results indicated that PKR activation in PAECs promotes the proliferation of PASMCs by triggering the release of HMGB1 and IL-1β, which promotes the proliferation of PASMCs and subsequently leads to the remodeling and muscularization of pulmonary arteries (Fig. 8).

Conclusion

This study first showed that that loss of PKR activity was sufficient to inhibit the development of pulmonary hypertension. Endothelial PKR promotes inflammatory release via ASC activation to induce pulmonary vascular remodeling, which is an important initiating event of PH. These conclusions were based on the following results: (i) PKR activity was increased in experimental MCT- and SuHx-PH models; (ii) chemical inhibition or genetic ablation of PKR inhibited the development of PH, which was accompanied by inactivation of the inflammasome adaptor ASC and inhibition of HMGB1 and IL-1β release; (iii) Deletion of ASC is effective in attenuating the development of PH in SuHx models; (iv) knockout of ASC inhibits the release of HMGB1 and IL-1β and (v) silencing PKR in PAECs was

sufficient to abolish the abnormal proliferation of PASMCs by blocking the release of HMGB1 and IL-1β.

The pathogenesis of PH is complex and multifactorial. Although the molecular and cellular mechanisms that initiate and perpetuate vascular remodeling, especially abnormal PASMC proliferation, remain unclear, some features have been shared in PH patients and animal models. Increased inflammatory infiltration is a typical trait of PH, and inhibiting inflammatory cytokines, including IL-1β, HMGB1 and TNF-α, can prevent the development of PH.[7,24,25] PKR is an important molecule of inflammatory-sensing pathways.[13] In this study, we found that PKR was specifically activated in the endothelial cell of pulmonary vessels in two different experimental PH models. In vitro, the pro-PH factor TNF-α also induced PKR activation in PAECs. Similar with previous study that TNF-α induces PKR activation in brain of Alzheimer patients.[26] Our results suggested that TNF-α is also a pro-activation factor of PKR in pulmonary arterial vessels. Since the pulmonary arterial endothelial dysfunction is the initial factor of PH, and the expression and activation of PKR is mainly concentrated in pulmonary arterial endothelium, PKR is likely to participate in the occurrence of PH. In our study, PKR inhibitor or PKR knockout both significantly prevented the development of SuHx-induced PH and inflammatory infiltration. These results demonstrated that PKR promotes inflammatory infiltration to play a crucial role in the pathogenesis of PH.

PKR promotes the release of inflammatory factors through combination with inflammasome to recruit ASC. ASC, as an indispensable inflammasome adaptor, is important for the activation of inflammasomes, including NLRP3, NLRC4, AIM2 and NLRP9b, which then recruits the inflammatory protease caspase-1 to release IL-1β and HMGB1.[27] However, previous studies have shown that knockout of NLRP3, NLRC4, AIM2 or NLRP9b alone failed to effectively inhibit the occurrence of experimental PH, whereas experimental hypoxia PH can be inhibited in ASC-deficient mice.[19] This phenomenon is probably due to ASC-mediated activation of various inflammasomes. In line with PKR deletion mice, ASC knockout mice moderated the increase in right ventricle systolic pressure (RVSP) and RV remodeling relative to wild-type controls.

However, the role of endothelial PKR and ASC on PH needed to be further demonstrated. In our animal models, the global knockout of PKR and ASC do not completely mimic the effect of PKR on PH models. In addition, we cannot exclude whether PKR and ASC on other cell types also induce a potential effect on PH. Innate immune cells also associated with the development of PH. Abnormal macrophages, T cells, B cells and dendritic cells are prominent in advanced obliterative plexiform lesions and occlusive pulmonary arteries remodeling observed in experimental and clinical PH.[28] Due to PKR and ASC have long been verified to promote inflammatory factors

release in immune cell,[17,29] whether the pro-inflammatory role of PKR and ASC on immune cells also induce the development of PH still need to further study.

This study also explains the reason that the levels of IL-1β and HMGB1 are increased in PH patients. The elevated activity of PKR possibly promoted the release of IL-1β and HMGB1 in PH patients, although we need further clinical experiments to prove. In addition, the elevated levels of IL-1β and HMGB1 can also be used as early biomarkers to confirm the occurrence of PH and activation of PKR in clinical patients.

In line with this finding, we found for the first time that deletion of PKR prevented PASMCs from excessive proliferation-induced vascular remodeling during PH development. The mechanism involved the inhibition of ASC activation, which decreased HMGB1 and IL-1β release. Our findings provide novel insights into PKR-mediated inflammatory and metabolic signaling in PH and might open a new avenue to treat vascular remodeling-associated cardiovascular diseases.

Authors' contribution

Yapei Li conceived and designed the experiments; Yapei Li, Lijun Li, Minghui Yin performed the experiments; Yapei Li, Ying Li, Jiangang Wang and Xiaohui Li analyzed the data; Yapei Li, Ying Li, Jiangang Wang and Xiaohui Li wrote and revised the paper. All authors read and approved the final article.

Guarantor

Yapei Li.

Conflict of interest

The author(s) declare that there is no conflict of interest.

Funding

ORCID iD

Xiaohui Li https://orcid.org/0000-0002-0624-8811

References

1. Thenappan T, Ormiston ML, Ryan JJ, et al. Pulmonary arterial hypertension: pathogenesis and clinical management. *BMJ* 2018; 360:j5492.
2. Southgate L, Machado RD, Graf S, et al. Molecular genetic framework underlying pulmonary arterial hypertension. *Nat Rev Cardiol* 2020; 17:85–95.

3. Weiss A, Neubauer MC, Yerabolu D, et al. Targeting cyclin-dependent kinases for the treatment of pulmonary arterial hypertension. *Nat Commun* 2019; 10: 2204.

4. Tian L, Wu D, Dasgupta A, et al. Epigenetic metabolic reprogramming of right ventricular fibroblasts in pulmonary arterial hypertension: a pyruvate dehydrogenase kinase-dependent shift in mitochondrial metabolism promotes right ventricular fibrosis. *Circ Res* 2020; 126:1723–1745.

5. Spiekerkoetter E, Kawut SM and de Jesus PV. New and emerging therapies for pulmonary arterial hypertension. *Annu Rev Med* 2019; 70: 45–59.

6. Ridker PM, Everett BM, Thuren T, et al. Antiinflammatory therapy with canakinumab for atherosclerotic disease. *N Engl J Med* 2017; 377:1119–1131.

7. Wang J, Tian XT, Peng Z, et al. HMGB1/TLR4 promotes hypoxic pulmonary hypertension via suppressing BMPR2 signaling. *Vascul Pharmacol* 2019; 117: 35–44.

8. Sharma RK, Oliveira AC, Kim S, et al. Involvement of neuroinflammation in the pathogenesis of monocrotaline-induced pulmonary hypertension. *Hypertension* 2018; 71: 1156–1163.

9. Li Y, Li XH, Yu ZX, et al. HIV protease inhibitors in pulmonary hypertension: rationale and design of a pilot trial in idiopathic pulmonary arterial hypertension. *Pulm Circ* 2015; 5: 538–546.

10. Feng W, Wang J, Yan X, et al. ERK/Drp1-dependent mitochondrial fission contributes to HMGB1-induced autophagy in pulmonary arterial hypertension. *Cell Prolif* 2021; 54: e13048.

11. Parpaleix A, Amsellem V, Houssaini A, et al. Role of interleukin-1 receptor 1/MyD88 signalling in the development and progression of pulmonary hypertension. *Eur Respir J* 2016; 48: 470–483.

12. Garcia-Ortega MB, Lopez GJ, Jimenez G, et al. Clinical and therapeutic potential of protein kinase PKR in cancer and metabolism. *Expert Rev Mol Med* 2017; 19: e9.

13. Kim Y, Park J, Kim S, et al. PKR senses nuclear and mitochondrial signals by interacting with endogenous double-stranded RNAs. *Mol Cell* 2018; 71: 1051–1063.

14. Liu CX, Li X, Nan F, et al. Structure and degradation of circular RNAs regulate PKR activation in innate immunity. *Cell* 2019; 177: 865–880.

15. Garcia-Ortega MB, Lopez GJ, Jimenez G, et al. Clinical and therapeutic potential of protein kinase PKR in cancer and metabolism. *Expert Rev Mol Med* 2017; 19: e9.

16. Li Y, Peng Z, Wang C, et al. Novel role of PKR in palmitate-induced Sirt1 inactivation and endothelial cell senescence. *Am J Physiol Heart Circ Physiol* 2018; 315: H571–H580.

17. Lu B, Nakamura T, Inouye K, et al. Novel role of PKR in inflammasome activation and HMGB1 release. *Nature* 2012; 488: 670–674.

18. Hett EC, Slater LH, Mark KG, et al. Chemical genetics reveals a kinase-independent role for protein kinase R in pyroptosis. *Nat Chem Biol* 2013; 9: 398–405.

19. Cero FT, Hillestad V, Sjaastad I, et al. Absence of the inflammasome adaptor ASC reduces hypoxia-induced pulmonary hypertension in mice. *Am J Physiol Lung Cell Mol Physiol* 2015; 309: L378–L387.

20. Yang J, Li X, Al-Lamki RS, et al. Smad-dependent and smad-independent induction of id1 by prostacyclin analogues inhibits proliferation of pulmonary artery smooth muscle cells in vitro and in vivo. *Circ Res* 2010; 107: 252–262.

21. Wang AP, Li XH, Gong SX, et al. miR-100 suppresses mTOR signaling in hypoxia-induced pulmonary hypertension in rats. *Eur J Pharmacol* 2015; 765: 565–573.

22. Li XW, Du J, Hu GY, et al. Fluorofenidone attenuates vascular remodeling in hypoxia-induced pulmonary hypertension of rats. *Can J Physiol Pharmacol* 2014; 92: 58–69.

23. Zurlo G, Piquereau J, Moulin M, et al. Sirtuin 1 regulates pulmonary artery smooth muscle cell proliferation: role in pulmonary arterial hypertension. *J Hypertens* 2018; 36: 1164–1177.

24. Hurst LA, Dunmore BJ, Long L, et al. TNF-alpha drives pulmonary arterial hypertension by suppressing the BMP type-II receptor and altering NOTCH signalling. *Nat Commun* 2017; 8: 14079.

25. Li Y, Li XH, Yu ZX, et al. HIV protease inhibitors in pulmonary hypertension: rationale and design of a pilot trial in idiopathic pulmonary arterial hypertension. *Pulm Circ* 2015; 5: 538–546.

26. Lourenco MV, Clarke JR, Frozza RL, et al. TNF-alpha mediates PKR-dependent memory impairment and brain IRS-1 inhibition induced by Alzheimer's beta-amyloid oligomers in mice and monkeys. *Cell Metab* 2013; 18: 831–843.

27. Place DE, Kanneganti TD. Recent advances in inflammasome biology. *Curr Opin Immunol* 2018; 50: 32–38.

28. Rabinovitch M, Guignabert C, Humbert M, et al. Inflammation and immunity in the pathogenesis of pulmonary arterial hypertension. *Circ Res* 2014; 115: 165–175.

29. Franklin BS, Bossaller L, De Nardo D, et al. The adaptor ASC has extracellular and 'prionoid' activities that propagate inflammation. *Nat Immunol* 2014; 15: 727–737.